Chemistry and Physics of Lipids 223 (2019) 104782

Contents lists available at ScienceDirect

Chemistry and Physics of Lipids

journal homepage: www.elsevier.com/locate/chemphyslip

Instrument response of phosphatidylglycerol lipids with varying fatty acyl chain length in nano-ESI shotgun experiments

Tommy Hofmann, Carla Schmidt*

Interdisciplinary research centre HALOmem, Charles Tanford Protein Centre, Institute for Biochemistry and Biotechnology, Martin Luther University Halle-Wittenberg, Kurt-Mothes-Str. 3a, 06120, Halle, Germany

ARTICLE INFO

Keywords:
Lipidomics
Nano-electrospray ionisation
Standard lipids
Quantification
Response factors
Calibration curve

ABSTRACT

In recent years, lipid quantification gained importance. In most cases, this is achieved by spiking the lipid mixture with deuterated standard lipids or lipid analogues that differ in chain length when compared with the natural lipid components. Usually, conventional ESI is employed requiring sample amounts which are not always available. Here, we evaluate the use of nano-ESI for accurate lipid quantification employing deuterated as well as short- and odd-fatty acyl chain analogues. We compare ionisation efficiencies of various phosphatidylglycerol species differing in fatty acyl chain length and saturation. While in our instrumental and experimental set-up differences in ionisation could not be observed for lipids varying in the number of double bonds, short-chain lipid species showed significantly higher intensities when compared with their long-chain analogues. To compensate for these differences and enable accurate quantification using short-fatty acyl chain lipid standards, we generated a calibration curve over a range of lipids with increasing chain length. We tested and evaluated the application of this calibration curve by comparison with a deuterated and odd-chain standard lipid for quantification of lipids in a mixture of known composition as well as a natural lipid extract. The different approaches deliver comparable quantities and are therefore applicable for accurate lipid quantification using nano-ESI. Even though generation of calibration curves might be more laborious, it has the advantage that peak overlap with natural lipids is eliminated and broad peak distributions of deuterated standards do not have to be assessed. Furthermore, it allows the calculation of response factors for long- or short-fatty acyl chain analogues when using deuterated or odd-numbered standard lipids for absolute quantification.

1. Introduction

Lipids are involved in many biological processes in which they serve as signalling, energy storage and membrane trafficking components. Biological membranes further separate the cell or cellular compartments from the outer environment thereby providing enclosed spaces for specific function. The lipid bilayer of these membranes mainly contains amphiphilic glycerophospholipids (often termed 'phospholipids'), which are composed of hydrophobic fatty acyl chains, a glycerol-phosphate backbone and in most cases a polar, hydrophilic head group. (Fahy et al., 2005, 2009) The head group defines the lipid class; examples are phosphatidylcholines, phosphatidylethanolamines, phosphatidylserines, phosphatidylglycerols (PG) and phosphatidylinositols. Phosphatidic acid, in contrast, is composed of two fatty acyl chains and glycerol-phosphate omitting the hydrophilic head group; it is therefore an important intermediate in glycerophospholipid production. (Athenstaedt and Daum, 1999) Each lipid class comprises various lipid species differing in length and saturation of each fatty acyl chain. (Yetukuri et al., 2008) In some cases, alkyl chains are linked by an ether bond forming so-called 'ether glycerolipids' which represent a large content of cell membranes in mammals and anaerobic bacteria. (Paltauf, 1994) The various lipid species include lipid isomers which have the same mass but differ in structure (e.g. PG 18:0_18:2 and PG 18:1/18:1) as well as lipid isobars which have the same nominal mass but differ in exact masses (e.g. PC 32:0 and PS 32:1). (Yergey et al., 1983)

In addition to phospholipids, sterols and sphingolipids are also components of biological membranes. (Harayama and Riezman, 2018) Sphingolipids are composed of a sphingoid base, an N-acyl chain and a head group which defines the subclass (i.e. ceramides, sphingomyelins or glycosphingolipids). Most sterols are derivatives of cholesterol. The lipid composition of cellular membranes defines its biophysical properties such as thickness, (Sharpe et al., 2010) curvature (Cooke and Deserno, 2006; McMahon and Boucrot, 2015) or protein-protein

* Corresponding author.
E-mail address: carla.schmidt@biochemtech.uni-halle.de (C. Schmidt).

https://doi.org/10.1016/j.chemphyslip.2019.05.007
Received 22 January 2019; Received in revised form 31 May 2019; Accepted 31 May 2019
Available online 06 June 2019

(Milovanovic et al., 2015; Schafer et al., 2011) and protein-lipid (Murray and Tamm, 2011; van den Bogaart et al., 2011) interactions. The knowledge of its exact composition is therefore of particular importance.

Lipidomics is a relatively young and fast-growing section of the *omics* technologies mostly applying mass spectrometry (MS) for the identification and quantification of a cellular lipidome. The identification of lipids by tandem MS is based on diagnostic fragment ions characteristic for the lipid class and species. (Schuhmann et al., 2012, 2011) There are two strategies commonly followed for lipid identification; first, direct infusion of the sample into the mass spectrometer (so-called 'shotgun' experiments), (Han and Gross, 2005) and second, separation of the lipids by liquid chromatography prior to MS analysis (LC–MS). (Cajka and Fiehn, 2014; Danne-Rasche et al., 2018) In early studies, one major drawback of shotgun lipidomics was strong ion suppression and the missing separation of isobaric species. However, the development of sensitive, high mass accuracy instrumentation nowadays allows the analysis of complex lipid mixtures including isobaric species in single shotgun experiments. (Schwudke et al., 2011)

Over the last decade, quantification of the lipidome gained importance and is often playing a role in clinical studies. (Shevchenko and Simons, 2010) Quantification in general is divided into two categories: First, relative quantification comparing the amounts of analytes across samples and thereby delivering a relative change mostly in form of a quantitative ratio and, second, absolute quantification yielding absolute amounts and concentrations of analytes in a sample. In lipidomics, quantification is usually performed by spiking the sample of interest with a suitable standard lipid corresponding to the class of interest. This standard lipid often contains deuterated fatty acyl chains causing a mass shift in the MS spectra. (Inloes et al., 2018) Similar to quantitative proteomics, the deuterated standard lipid features the same physicochemical properties as the natural analogues and, by spiking accurate amounts, allows obtaining quantitative values of the natural lipids from MS intensities. (Brugger et al., 1997; Lehmann et al., 1997) However, a shift in retention time during chromatographic separation has to be considered for deuterated lipids when compared with their endogenous analogues making shotgun approaches employing high-resolution instrumentation more favourable for these experiments.

A similar approach is the application of short- or long-fatty acyl chain analogues which, due to their different composition, also show a mass difference in the MS spectra. (Brugger et al., 1997) Similar to deuterated standard lipids they are added in known amounts followed by intensity-based quantification of lipids with natural chain length belonging to the same lipid class. Natural lipids in almost all animals contain mostly even-numbered fatty acyl chains. (Quehenberger et al., 2010) The addition of lipids containing odd-numbered fatty acyl chains therefore represents another possibility to obtain quantitative values based on the intensities within a lipid class. (Brugger et al., 1997; Koivusalo et al., 2001) One exception, however, is the lipidome of ruminant species which contains a large amount of odd-numbered fatty acyl chains in comparison with non-ruminant species. (Devle et al., 2012) In this case, deuterated standard lipids are the preferred choice.

In general, approaches utilising either deuterated standards or short-/long-/odd-fatty acyl chain analogues assume that the head group defines the response in the mass spectrometer while the fatty acid chain does not affect the ionisation process. However, there is evidence that the hydrophobicity, i.e. the length and saturation of the fatty acyl chain moiety, affects the ionisation efficiency and therefore the total intensity of the phospholipids. (Koivusalo et al., 2001) This evidence is based on conventional electrospray ionisation (ESI) at higher flow rates and at varying concentrations, while a comprehensive evaluation in nano-ESI is still missing. The application of nano-ESI, however, has the following advantages; smaller droplets of higher charge are produced facilitating the desolvation and ionisation process and thereby tolerating higher salt concentrations. (Juraschek et al., 1999; Wilm, 2011; Wilm and Mann, 1996) Importantly, smaller sample amounts are required which is of particular interest when studying crucial biological questions where samples are limited. Recently, the application of nano-ESI during LC–MS was optimised. (Danne-Rasche et al., 2018) Here, we compare the feasibility and accuracy of intensity-based lipid quantification using either deuterated standard lipids or short-/odd-fatty acyl chain analogues in nano-ESI MS. We further tested these approaches for quantification of a lipid mixture with known composition as well as a natural lipid extract.

2. Materials and methods

2.1. Lipids

The following lipid standards were employed:

1-palmitoyl-2-oleoyl-sn-glycero-3-phospho-(1′-rac-glycerol) (PG 16:0_18:1) (dissolved in Chloroform),

1-palmitoyl-d31-2-oleoyl-sn-glycero-3-[phospho-rac-(1-glycerol)] (PG 16:0(d31)_18:1) (dissolved in Chloroform),

1-palmitoyl-2-linoleoyl-sn-glycero-3-phospho-(1′-rac-glycerol) (PG 16:0_18:2) (dissolved in Chloroform),

1-stearoyl-2-oleoyl-sn-glycero-3-phospho-(1′-rac-glycerol) (PG 18:0_18:1) (dissolved in Chloroform),

1,2-distearoyl-sn-glycero-3-phospho-(1′-rac-glycerol) (PG 18:0/18:0) (lyophilized),

1,2-dioleoyl-sn-glycero-3-phospho-(1′-rac-glycerol) (PG 18:1/18:1) (dissolved in Chloroform),

1,2-dilinoleoyl-sn-glycero-3-phospho-(1′-rac-glycerol) (PG 18:2/18:2) (dissolved in Chloroform),

1,2-dilinolenoyl-sn-glycero-3-phospho-(1′-rac-glycerol) (PG 18:3/18:3) (dissolved in Chloroform),

1,2-dihexanoyl-sn-glycero-3-phospho-(1′-rac-glycerol) (PG 6:0/6:0) (lyophilized),

1,2-dioctanoyl-sn-glycero-3-phospho-(1′-rac-glycerol) (PG 8:0/8:0) (lyophilized),

1,2-didecanoyl-sn-glycero-3-phospho-(1′-rac-glycerol) (PG 10:0/10:0) (dissolved in Chloroform),

1,2-dilauroyl-sn-glycero-3-phospho-(1′-rac-glycerol) (PG 12:0/12:0) (lyophilized),

1,2-dimyristoyl-sn-glycero-3-phospho-(1′-rac-glycerol) (PG 14:0/14:0) (lyophilized),

1,2-dipalmitoyl-sn-glycero-3-phospho-(1′-rac-glycerol) (PG 16:0/16:0) (lyophilized),

1,2-diheptadecanoyl-sn-glycero-3-phospho-(1′-rac-glycerol) (PG 17:0/17:0) (lyophilized),

1-dodecanoyl-2-tridecanoyl-sn-glycero-3-phospho-(1′-rac-glycerol) (PG 12:0_13:0) (dissolved in Methanol),

1-palmitoyl-2-docosahexaenoyl-sn-glycero-3-phospho-(1′-rac-glycerol) (PG 16:0_22:6) (dissolved in chloroform)

L-α-phosphatidylglycerol (Egg, Chicken) (egg PG) (dissolved in Chloroform).

All lipid standards were purchased from Avanti Polar Lipids Inc. (Alabaster, USA). Aliquots of defined concentration were prepared from lipids available in chloroform followed by evaporation of the solvent under a stream of nitrogen. Lipids available as powder (lyophilized) were first dissolved in chloroform followed by preparation of aliquots and evaporation of the solvent. Lipid concentrations were confirmed by phosphate analysis.

The lipid shorthand nomenclature proposed by Liebisch et al. (2013) was used throughout the manuscript. Accordingly, phospholipids are abbreviated by their lipid class followed by number of C-atoms:number of double bonds (e.g. PG 34:1). If the fatty acids and the *sn*-position are known, they are listed as *sn1/sn2*. If the *sn*-position is unknown, the fatty acyl chains are separated by "_" (e.g. PG 16:0_18:1). As the mass spectrometric techniques employed in this study do not provide insights into the *sn*-position of the various lipid species, we have used the latter notation unless the *sn*-positions are unambiguous.

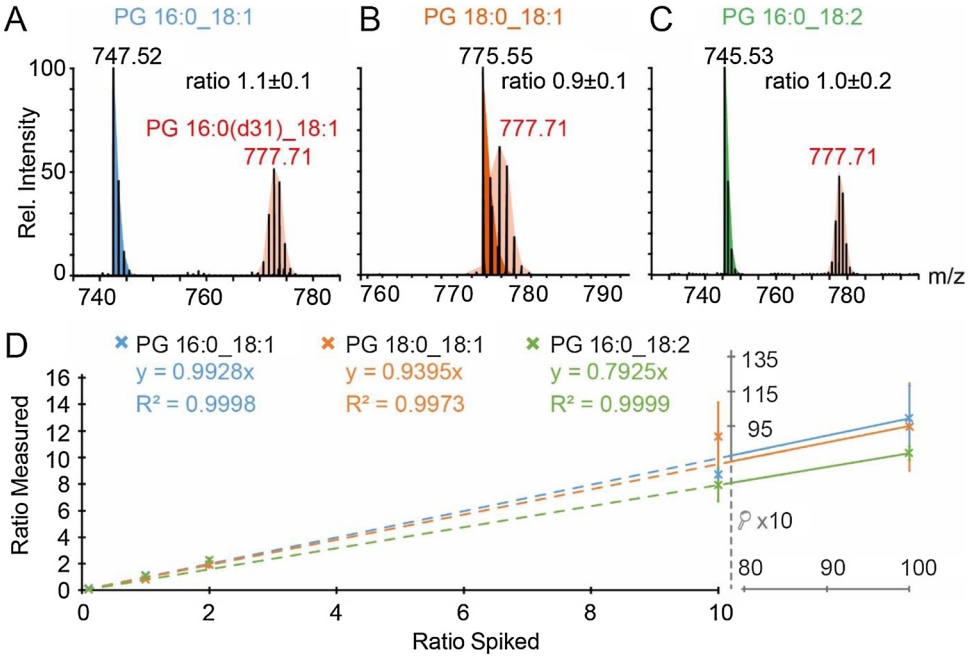

Fig. 1. Quantification of PG lipids using a deuterated standard lipid, namely PG 16:0(d31)_18:1. Three different PG species were spiked with PG 16:0(d31)_18:1 in equal amounts. Intensity ratios were then obtained from integrated peak areas. **(A)** PG 16:0_18:1, **(B)** PG 18:0_18:1, **(C)** PG 16:0_18:2. **(D)** Linearity of quantification was assessed. Various mixing ratios ranging from 1:10 up to 100:1 were mixed and observed ratios were plotted against theoretical ratios. For all lipid species linear regression was observed ($R^2 > 0.997$). Absolute intensities of accumulated mass spectra: 1.13E + 09 (A), 6.26E + 08 (B), 1.09E + 09 (C). Note that relative abundance ratios were used for quantification.

2.2. Chemicals

All solvents were purchased at Sigma-Aldrich (St. Louis, USA) and were at least HPLC grade. Other chemicals were also purchased at Sigma-Aldrich with highest purity available.

2.3. Lipid quantification using deuterated or short-fatty acyl chain analogues

Stock solutions of lipids were prepared as described above. For lipid quantification, 1 mmol of each lipid were dissolved in chloroform and diluted with methanol and water to a final concentration of 10 µM in 70% (v/v) methanol, 25% (v/v) water, 5% (v/v) chloroform (final volume 100 µl). All lipids were analysed by direct infusion on a Q Exactive Plus Hybrid Quadrupole-Orbitrap mass spectrometer (Thermo Fisher Scientific, Bremen, Germany) equipped with a Nanospray Flex ion source (Thermo Fisher Scientific, Bremen, Germany). 2–3 µl were loaded into a borosilicate offline emitter coated with gold/palladium (Thermo Fisher Scientific). In our source set-up, the flow-rate was estimated to be 100–150 nl/min.

MS settings were: capillary voltage, -2 to 2.8 kV; capillary temperature, 250 °C; resolution, 70.000; RF-lens level, 60. Mass spectra were recorded in negative ion mode with the following parameters: max injection time, 100 ms; automated gain control, $2{\cdot}10^6$; microscans, 1. MS scan range was 150-1000 *m/z*. For quantification, scans of approx. 3 min. were accumulated. Peak areas were then integrated over four isotopic peaks obtained in the mass spectra. Lipids were quantified by calculating abundance ratios from these peak areas.

2.4. Lipid quantification of lipid species with overlapping isotope distribution

When isotope distributions of lipid species with varying number of double bonds overlapped, we made use of the theoretical isotope pattern of lipids and first extracted isotope distributions for each lipid species in the defined *m/z* range (i.e. the overlapping *m/z* area). Here, the total peak intensity is the sum of all peak intensities of individual lipid species. The sum of the peak intensities of each *m/z* value consequently results in the experimentally observed mass spectrum. Next, peak areas were integrated over four isotopic peaks and the various lipid species were quantified by calculating abundance ratios. The quantification workflow is shown in **Figure S1A**. Extracting the isotope distributions for all lipid species in the *m/z* region allows calculating the relative proportion of each individual lipid species (**Figure S1B**).

3. Results and discussion

3.1. Lipid quantification using deuterated standard lipids

To achieve accurate lipid quantification and, at the same time, unambiguous identification of lipid species including their isobars, we employed a Q Exactive plus mass spectrometer. This mass spectrometer provides high mass accuracy and resolution, and therefore allows direct infusion of even complex lipid mixtures. To establish a platform for the analysis of lipids from limited sample amounts, we employed nano-ESI instead of conventional ESI. We first evaluated the fragmentation characteristics of several lipid classes and found that comparable fragment ions were observed as published previously for conventional ESI shotgun experiments (data not shown). (e.g. Schuhmann et al., 2011; Han and Gross, 2005; Godzien et al., 2015; Han and Gross, 1995)

Before establishing PG quantification, we evaluated possible in-source fragmentation in our experimental set-up. We found that intensities of fragment ions were < 5% when compared with the precursor ion and therefore assume that accurate quantification of PG lipids is possible in an acceptable range of error. In a first experiment, we spiked a PG species (PG 16:0_18:1) with the same amount of its deuterated analogue (i.e. PG 16:0(d31)_18:1) and subsequently analysed the lipid mixture in nano-ESI shotgun experiments. The two lipid species were observed at *m/z* 747.52 (PG 16:0_18:1) and *m/z* 777.71 (PG 16:0(d31)18:1) with isotopic peak distributions characteristic for natural as well as deuterated lipid species (Fig. 1A). Of note, the deuterated lipid shows a broader isotope distribution than non-deuterated lipids caused by incomplete deuteration of the fatty acyl chain. We calculated the intensity ratio of the two lipids by integrating their peak areas (**Methods**). The observed ratio of 1.10 ± 0.1 is close to the theoretical value of 1.00 showing the potential of using deuterated standard lipids for quantification.

We next studied the effect of chain length and saturation, i.e. the number of double bonds, on this intensity-based quantification approach. For this, we employed a lipid species containing a C2-unit

longer fatty acyl chain with the same number of double bonds (PG 18:0_18:1) (Fig. 1B) as well as a standard lipid containing the same fatty acyl chains but an additional double bond (PG 16:0_18:2) (Fig. 1C). Both lipid species were spiked with equal amounts of the deuterated standard lipid (PG 16:0(d31)_18:1) and analysed as described. Intensity ratios of 0.9 ± 0.1 for PG 18:0_18:1 *versus* PG 16:0(d31)_18:1 and 1.0 ± 0.2 for PG 16:0_18:2 *versus* PG 16:0(d31)_18:1 were calculated from obtained peak areas, respectively. For both lipids, intensity ratios close to the theoretical value were obtained showing that an additional double bond or C2-unit in the fatty acyl chain only minimally affect intensity-based quantification.

Linearity of this approach was then tested for the three PG species employed here. For this, the three lipids were spiked with the deuterated standard (PG 16:0(d31)_18:1) in varying mixing ratios ranging from 1:10 up to 100:1 (Fig. 1D). Measured intensity ratios for all three lipids correlate well with the spiked ratios as revealed by linear regression analysis ($R^2 > 0.997$). Employing deuterated lipid standards for quantification of similar lipid species therefore represents a promising application over a wide concentration range. However, as observed in the respective mass spectra (Fig. 1**A–C**), a broader peak distribution of the deuterated lipid has to be considered when integrating peak areas for quantification.

3.2. Assessing the effects of fatty acyl chain unsaturation

Having assessed the effect of small changes in the fatty acyl chain composition, we set out to evaluate major variations such as higher numbers of double bonds (zero up to six double bonds). In previous studies, acyl chain saturation was found to have a significant effect on the instrument response in ESI experiments, however, this diminished with progressive dilution. (Koivusalo et al., 2001) We assessed the effect of unsaturation in our instrumental and experimental set-up employing nano-ESI and a water-containing solvent system (i.e. 70% (v/v) Methanol, 25% (v/v) Water, 5% (v/v) Chloroform). For this, we compared four lipid species, namely PG 18:0/18:0, PG 18:1/18:1, PG 18:2/18:2 and PG 18:3/18:3. These four lipid species were mixed in equal amounts and analysed by shotgun analysis (**Methods**). Due to the addition of two double bonds per lipid species, their isotope envelopes do not overlap in their mass spectra allowing for unambiguous comparison of their peak areas (Fig. 2A). Indeed, the four lipids were obtained at *m/z* 765.47 (PG 18:3/18:3), *m/z* 769.50 (PG 18:2/18:2), *m/z* 773.54 (PG 18:1/18:1) and *m/z* 777.57 (PG 18:0/18:0) showing the full isotope distribution for each lipid (Fig. 2A).

As the four lipid species used here contain the same number of carbon atoms in both fatty acyl chains (i.e. two C18-fatty acyl chains) and only differ in the number of double bonds, their intensities can directly be compared and possible effects can be attributed to acyl chain saturation rather than fatty acyl chain length. In contrast to previous studies, (Koivusalo et al., 2001) the intensities of all four species were comparable in this mass spectrum at fairly high lipid concentration (10 μM total lipid concentration). The average relative intensities varied for all four species between 84 and 100% in three independent replicates (Fig. 2A**, panel ii**). These differences originate most likely from mixing errors. We next analysed the same lipid mixture at lower concentration (1 μM and 0.1 μM total lipid concentration) as well as differing mixing ratios (not shown). In all cases, observed intensities reflected the mixing ratios.

We further tested two other lipids with overlapping isotope distribution, namely PG 16:0_18:2 and 16:0_18:1. These two lipids were mixed in equal amounts at different total lipid concentration (Fig. 2B). As before, after applying our quantification strategy described (**Figure S1**), we find that both lipids show comparable intensities (Fig. 2B).

We conclude that the number of double bonds (up to six in these examples) does not affect the ionisation efficiency in our experimental set-up. Possible explanations are the generation of smaller nano-ESI droplets or the water-containing solvent system used here. Unsaturated lipids are expected to have a higher surface activity than their saturated analogues, however, as no differences were observed in our measurements, we assume that these differences are within the error range and therefore unnoticed in our measurements.

3.3. Quantification using short-fatty acyl chain lipid analogues

We next varied the fatty acyl chain length. For this we chose significantly shorter fatty acyl chains such as hexanoyl chains (C_6) up to naturally abundant fatty acyl chains such as oleoyl chains (C_{18}). By choosing PG lipids which differ by C2-units we obtained a complete series of lipid species ranging from PG 6:0/6:0 up to PG 18:0/18:0. We also included one odd-numbered fatty acyl chain lipid, namely PG 17:0/17:0.

These eight lipid species were mixed in equal amounts (resulting in a total lipid concentration of 10 μM) and analysed by shotgun lipidomics. We found that lipid species with shorter fatty acyl chains showed significantly higher intensities in the mass spectra when compared with the lipid species containing longer fatty acyl chains (Fig. 3A). To avoid effects of ion suppression when analysing the complete series of lipid species, we also spiked every individual lipid species with the deuterated standard lipid used above (i.e. PG 16:0(d31)_18:1) and analysed them separately (**Figure S2**). Nonetheless, when comparing the relative intensities of each lipid species with the deuterated standard, we obtained intensity differences in the same range as for the analysis of all lipid species in the same experiment (**Figure S2** and Fig. 3).

To allow quantification using short-fatty acyl chain analogues, we made use of the intensity differences observed for the series of lipids with different chain length and generated a calibration curve by exponentially fitting observed intensities (Fig. 3B). This calibration curve should in principle allow the calculation for response factors of any lipid species in the range employed here (i.e. PG 6:0/6:0 up to PG 18:0/18:0). To test this hypothesis, we employed three mixed acyl chain lipids which were not used to establish the calibration curve, namely PG 12:0_13:0, PG 16:0_18:1 and PG 16:0_22:6. All lipids were mixed in equal amounts (10 μM total lipid concentration) with the shortest fatty acyl chain variant (PG 6:0/6:0) which showed the highest relative intensity of all lipids. The relative intensities of the lipids were then compared with the theoretical values of the calibration curve corresponding to their number of carbon atoms. Indeed, the relative intensities showed values close to the predicted values (**Figure S3**).

3.4. Quantification of a lipid mixture with known composition using a deuterated standard lipid and short-/odd-fatty acyl chain analogues

Having evaluated the quantification of lipids using a similar deuterated lipid analogue as well as having established a calibration curve enabling the application of short-fatty acyl chain analogues, we set out to quantify a lipid mixture of known composition. For this, we prepared a mixture containing five PG species in known quantities: PG 16:0/16:0 (1 μM), PG 16:0_18:1 (1 μM), PG 18:1/18:1 (2 μM), PG 18:0_18:1 (1 μM) and PG 18:0/18:0 (1.2 μM). We spiked this lipid mixture with three standard lipids, namely PG 6:0/6:0, PG 17:0/17:0 and PG 16:0(d31)_18:1, each at 1 μM concentration. The spectrum shows all lipid species at reasonable intensities (Fig. 4A).

Following the strategies described above, we were able to quantify the five PG lipids. For comparison, we also quantified the spiked PG 17:0/17:0 standard when using PG 6:0/6:0 or PG 16:0(d31)_18:1 for quantification. The obtained quantities are close to the theoretical values for all quantification strategies (Fig. 4B). Importantly, when using short-chain lipid analogues for intensity-based quantification without applying the established calibration curve, quantitative values differed significantly (**Figure S4**) highlighting the need of a calibration curve compensating for differences during MS measurements and allowing the calculation of response factors in the range of the calibration curve.

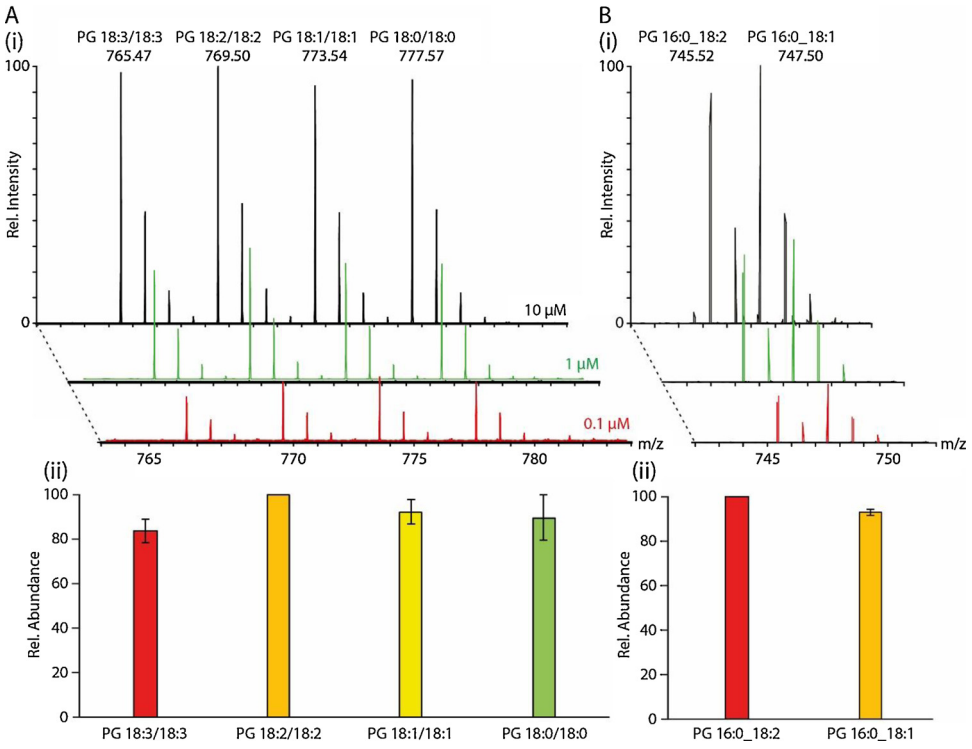

Fig. 2. The effect of number of double bonds on lipid ionisation. Two series of PG species differing in the number of double bonds were employed: (A) PG 18:3/18:3 (*m/z* 765.47), PG 18:2/18:2 (*m/z* 769.50), PG 18:1/18:1 (*m/z* 773.54) and PG 18:0/18:0 (*m/z* 777.57) and (B) PG 16:0_18:2 (m/z 745.52) and 16:0_18:1 (m/z 747.50). **(A)** Mass spectrum of a 1:1:1:1 mixture of all four PG species (10 µM total lipid concentration). Due to the increment of two double bonds per species the observed isotope distributions do not overlap in the mass spectrum. Mass spectra of the same lipid mixture at 1 µM (green) and 0.1 µM (red) are shown. Of note, the intensity range for diluted samples is not scaled (panel i). The lipid mixture was analysed in several replicates (n = 3) The average relative intensities for all four species are plotted. PG 18:2/18:2 displayed highest intensities in all measurements. Intensities of the other lipids are shown relative to PG 18:2/18:2 (panel ii). **(B)** Mass spectrum of a 1:1 mixture of two PG species (10 µM total lipid concentration). Due to the increment of one double bond, the observed isotope distributions overlap in the mass spectrum. Mass spectra of the same lipid mixture at 1 µM (green) and 0.1 µM (red) are shown. Of note, the intensity range for diluted samples is not scaled (panel i). The lipid mixture was analysed in three replicates (n = 3) The average relative intensities of the two species are plotted. PG 16:0_18:2 showed highest intensities. Intensities of PG 16:0_18:1 is shown relative to PG 16:0_18:2 (panel ii). Absolute intensities of accumulated mass spectra: 3.28E + 07 (A), 2.46E + 07 (B). Note that relative abundance ratios were used for quantification.

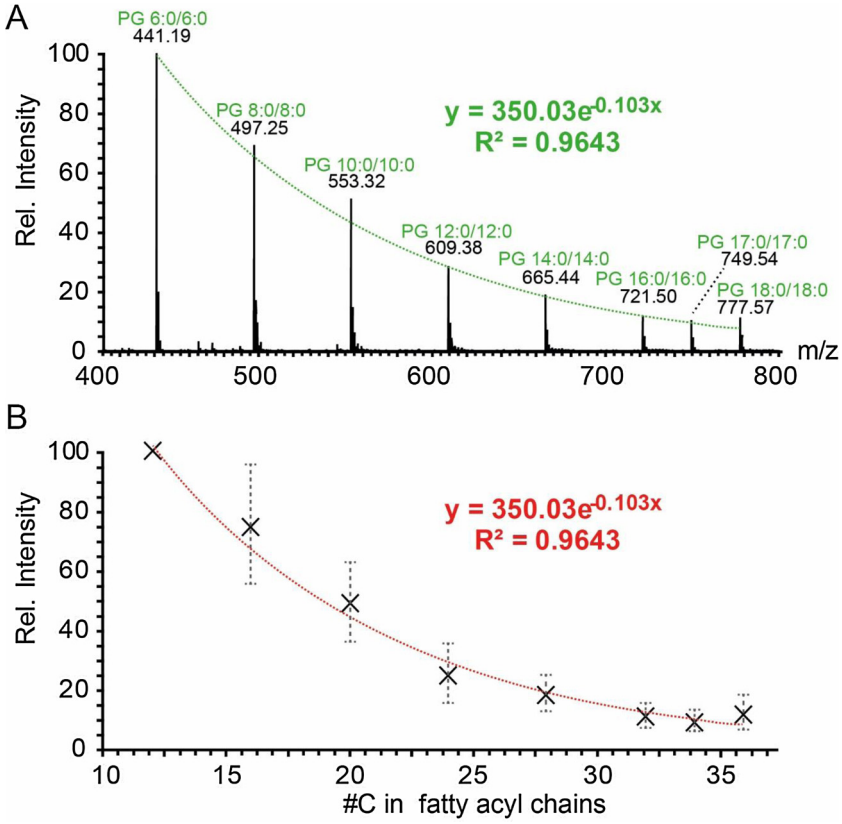

Fig. 3. Calibration curve for quantification using short-fatty acyl chain analogues. A series of PG species with varying fatty acyl chain length was employed ranging from PG 6:0/6:0 up to PG 18:0/18:0. PG 17:0/17:0 was also included. **(A)** All lipids were mixed in equal amounts (10 µM total lipid concentration) and analysed in the same mass spectrum (n = 6). Absolute intensity of the accumulated mass spectrum: 8.92E + 07. Note that relative abundance ratios were used for generation of the calibration curve. **(B)** A calibration curve and equation was obtained from exponential fitting of the relative intensities.

Using PG 17:0/17:0 and PG 16:0(d31)_18:1 allows quantification of PG species by simply comparing observed peak intensities while short-chain analogues require further data processing by applying the established calibration curve. Nonetheless, short-fatty acyl chain analogues can successfully be employed for quantification when the calibration curve reflects the instrument response (Fig. 4). Of note, as

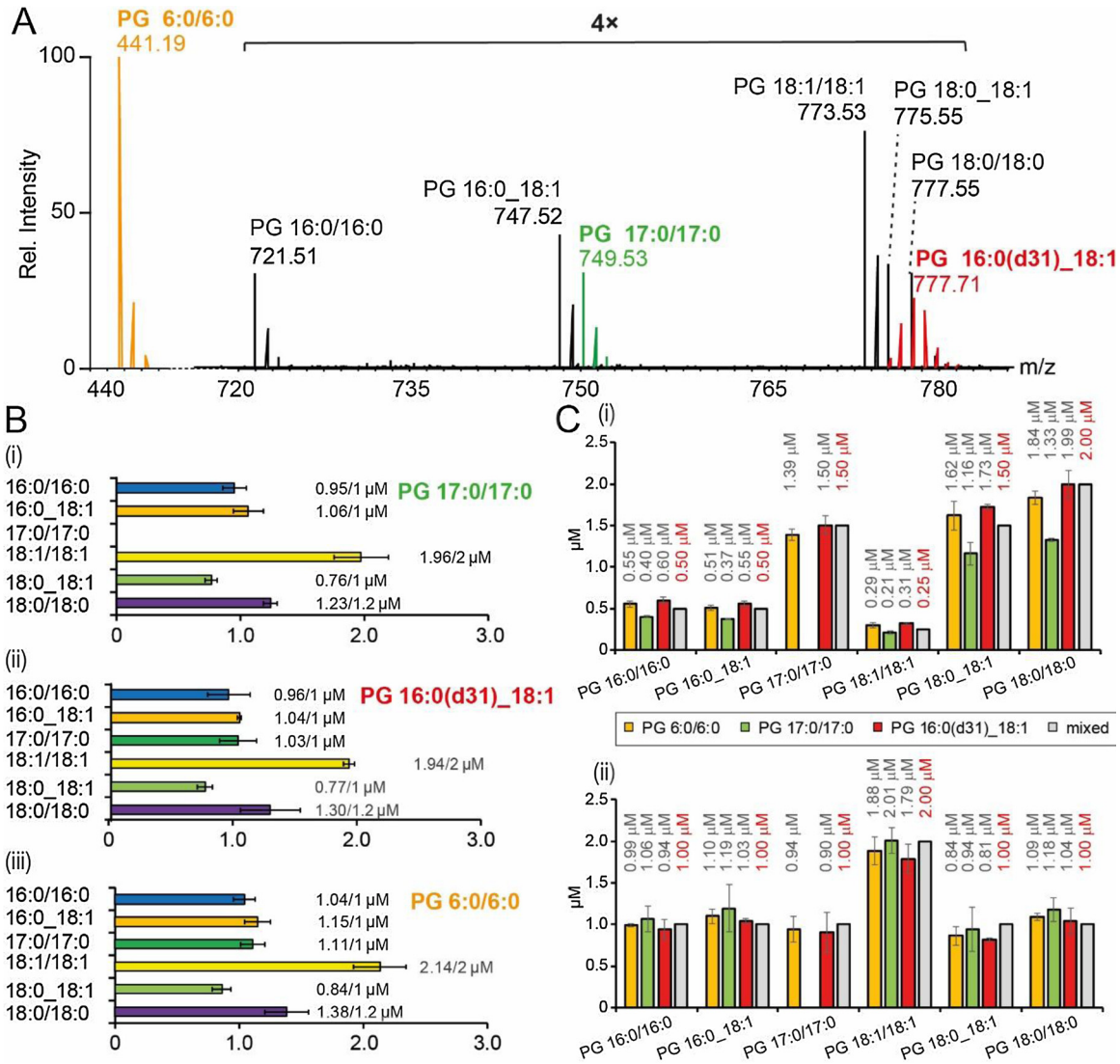

Fig. 4. Quantification of a lipid mixture with known composition using a deuterated standard lipid as well as odd- and short-fatty acyl chain analogues. **(A)** Mass spectrum observed. The five PG lipids as well as PG 6:0/6:0 (yellow), PG 17:0/17:0 (green) and PG 16:0(d31)/_18:1 (red) were observed. The total lipid concentration is 9.2 µM resulting from individually spiked lipid species. Absolute intensity of accumulated mass spectrum: 2.85E + 07. Note that relative abundance ratios were used for quantification. **(B)** The lipids were quantified by comparing integrated peak areas of standard lipids versus mixed PG lipids (panels i and ii). The calibration curve was applied to compensate for differences in intensities between short-fatty acyl chain analogues and natural lipid species (iii). **(C)** Quantification of a lipid mixture with 8.25 µM (i) and 9 µM (ii) total lipid concentration.

shown above, deuterated standard lipids show a broader isotope distribution and integration of peak areas has to be adjusted.

We also prepared two other lipid mixtures containing the same PG lipids albeit at different quantities. Again, the obtained quantities agree well among the different quantification strategies (Fig. 4C).

3.5. Quantification of a natural lipid mixture (egg PG) using a deuterated standard lipid and short-/odd-fatty acyl chain analogues

Having evaluated lipid quantification using deuterated lipid standards as well as short-/odd-fatty acyl chain analogues, we now set out to apply these approaches to a sample from natural sources. For this we employed egg PG, a lipid mixture of several PG species extracted from chicken egg. The lipid mixture was spiked with (i) PG 6:0/6:0 and PG 8:0/8:0 (not shown), (ii) PG 17:0/17:0 and (iii) PG 16:0(d31)_18:1, the deuterated standard lipid used above. The respective mass spectrum shows peak distributions for the three spiked lipids standards as well as several PG species of which PG 16:0_18:2, PG 16:0_18:1, PG 18:0/18:0, PG 18:1/18:1, PG 18:1_18:2 and PG 18:2/18:2 are most abundant (Fig. 5A).

For all detected lipid species, peak areas were determined as described (**Methods**). For overlapping species, i.e. PG 16:0_18:2 and PG 16:0_18:1 as well as PG 18:0/18:0, PG 18:1/18:1, PG 18:1_18:2 and PG 18:2/18:2, theoretical isotope distributions were first calculated to allow determination of individual peak areas (see **Methods** and **Figure S1** for details). All PG species were quantified by comparing the peak areas of the individual species with those obtained for the deuterated and the odd-numbered standard lipids (Fig. 5B). In addition, the various species were also quantified by making use of the calibration curve established above using the short-chain analogue PG 6:0/6:0 or PG 8:0/8:0 (Fig. 5B). In all cases, similar quantitative values were obtained and the absolute amounts of the individual lipid species reflect the intensities observed in the mass spectrum (Fig. 5). Our comparison therefore shows that the three quantification approaches followed here are comparable when analysing natural lipid extracts. Again, when employing short-chain lipid analogues for lipid quantification without applying the established calibration curve, quantities differed significantly from the obtained values (**Figure S5**).

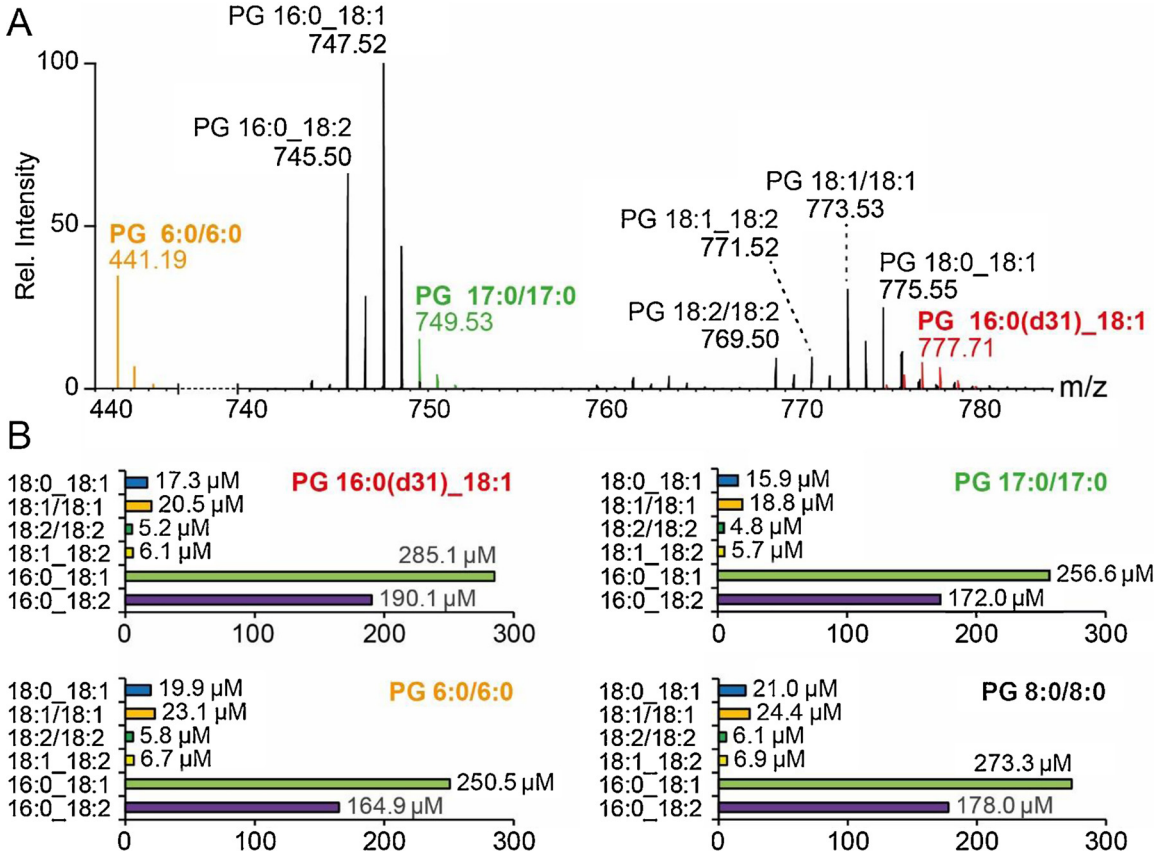

Fig. 5. Quantification of lipids in egg PG using a deuterated standard lipid as well as odd- and short-fatty acyl chain analogues. (A) Mass spectrum obtained from egg PG. Various PG species were observed in the mass spectrum. The lipid extract was spiked with PG 6:0/6:0 (yellow), PG 8:0/8:0 (not shown), PG 17:0/17:0 (green) and PG 16:0(d31)/_18:1 (red). All standard lipids were spiked in equal amounts (i.e. 10 µM each). Absolute intensity of the accumulated mass spectrum: 1.11E + 08. Note that relative abundance ratios were used for quantification. **(B)** The lipids were quantified by comparison of the integrated peak areas of natural lipids versus those of standard lipids. The calibration curve was applied to compensate for differences in intensities between short-fatty acyl chain analogues (PG 6:0/6:0 and PG 8:0/8:0) and natural lipid species.

An important aspect when quantifying lipid extracts from biological samples is, however, the choice of the extraction method. Different extraction protocols employing methanol and chloroform, (Bligh and Dyer, 1959; Folch et al., 1957) hexane and isopropanol (Hara and Radin, 1978) or methanol and methyl-tert-butyl ether (Matyash et al., 2008) are available and have been compared for lipidomic studies. (Reis et al., 2013) While all procedures delivered comparable results for predominant lipid classes, the choice of extraction method is more important for low abundant lipid classes such as PIs and should carefully be considered. (Han et al., 2006) In addition, differences in extraction of lipid species differing in fatty acyl chain length have to be considered when spiking samples from natural sources with standard lipids before extraction.

4. Conclusion

In this study we assessed MS-based lipid quantification using nano-ESI. We evaluated and compared the application of deuterated lipid standards as well as short- and odd-fatty acyl chain analogues. We found that the length of the fatty acyl chain significantly effects the ionization efficiency, however, these differences can be compensated for by employing a calibration curve generated from lipid species with varying chain length. Differences in fatty acyl chain saturation were not observed in our experimental set-up. In nano-ESI, differences in instrument response were independent on the concentration employed (**Figure S6**). In conventional ESI, however, differences in ionization efficiency were observed for both, lipids differing in fatty acyl chain length and saturation. (Koivusalo et al., 2001; Han et al., 2006) These effects were concentration dependent and diminished with progressive dilution. One possible explanation for these differences is that release of ions in ESI and nano-ESI depends on droplet fission and compounds with higher surface activity have a better chance to be transferred to the next generation droplet. (Schmidt et al., 2003) Larger initial droplets as observed in ESI require higher number of fission events allowing compounds differing in surface activity being transferred in parallel fission cascades. Dilution of samples can therefore diminish effects of surface activity. For smaller droplets, as observed in nano-ESI, surface activity is more relevant causing differences in ion intensity for lipids with varying fatty acyl chain length. Due to the relatively small size of droplets, dilution of samples does not eliminate these effects in the comparably short fission cascades. Therefore, differences in instrument response remain when analysing diluted samples using nano-ESI. Surprisingly, differences in ionization efficiency were not observed for lipids differing in saturation of fatty acyl chains. We assume that the differences in surface activity are comparably small and the differences in ionization lie within the range of error. This agrees well with the small differences in instrument response observed for PG species with longer fatty acyl chains (i.e. PG 14:0/14:0, PG 16:0/16:0, PG 17:0/17:0 and PG 18:0/18:0). To test this hypothesis, PG species with unsaturated, short fatty acyl chains (if available) should be evaluated.

Using short-fatty acyl chain lipids and generating a calibration curve for quantification of lipids when using nano-ESI, rather than spiking deuterated or odd-fatty acyl chain analogues, has the following advantages: (i) Isotope distributions of the standard lipid and the naturally found lipids do not overlap; (ii) Isotope envelopes of deuterated standard lipids, which can differ depending on the degree of

deuteration, do not need to be evaluated; (iii) Odd-fatty acyl chain lipids might be components of the natural lipid extract/mixture and would be overlooked when spiking odd-fatty acyl chain analogues. However, the instrument response might differ for the various MS systems available and the calibration curve needs to be generated for every individual system. In addition, the calibration curve should be recorded for the concentration range of the lipids under investigation. Nonetheless, generating a calibration curve as suggested in this study provides insights into the instrument response of every individual system and allows calculation of response factors. These prove particularly helpful when quantifying lipids from natural sources using standard lipids with defined chain length which do not cover the full range of available lipid species. In these cases, response factors will enable quantification of short or long fatty acyl chain analogues.

Previous studies almost exclusively employed PC lipids in positive ion mode to study the effects of ionization and instrument response. Here, we used PG lipids; mainly because the complete lipid series ranging from PG 6:0/6:0 up to 18:0/18:0 is commercially available at reasonable purity. This includes odd-chain analogues as well as lipids that differ in fatty acyl chain saturation. In addition, PG lipids are best analyzed in negative ion mode which is often applied in lipidomic analyses of phospholipids. Employing PG for a systematic evaluation of the different quantification approaches therefore contributes to the established workflows and applications. Nonetheless, these experiments should be repeated for other lipid classes and species to characterize the full spectrum of naturally occurring lipids. This venture, however, clearly depends on the availability of pure standard lipids.

Funding

This work was supported by the Federal Ministry for Education and Research (BMBF, ZIK programme, 03Z22HN22), the European Regional Development Funds (EFRE, ZS/2016/04/78115) and the Martin Luther University Halle-Wittenberg.

Acknowledgements

We thank Julian Bender and Melissa Frick for critically reading the manuscript.

Appendix A. Supplementary data

Supplementary material related to this article can be found, in the online version, at doi:https://doi.org/10.1016/j.chemphyslip.2019.05.007.

References

Athenstaedt, K., Daum, G., 1999. Phosphatidic acid, a key intermediate in lipid metabolism. Eur. J. Biochem. 266 (1), 1–16.
Bligh, E.G., Dyer, W.J., 1959. A rapid method of total lipid extraction and purification. Can. J. Biochem. Physiol. 37 (8), 911–917.
Brugger, B., Erben, G., Sandhoff, R., Wieland, F.T., Lehmann, W.D., 1997. Quantitative analysis of biological membrane lipids at the low picomole level by nano-electrospray ionization tandem mass spectrometry. Proc Natl Acad Sci U S A 94 (6), 2339–2344.
Cajka, T., Fiehn, O., 2014. Comprehensive analysis of lipids in biological systems by liquid chromatography-mass spectrometry. Trends Analyt. Chem. 61, 192–206.
Cooke, I.R., Deserno, M., 2006. Coupling between lipid shape and membrane curvature. Biophys. J. 91 (2), 487–495.
Danne-Rasche, N., Coman, C., Ahrends, R., 2018. Nano-LC/NSI MS refines lipidomics by enhancing lipid coverage, measurement sensitivity, and linear dynamic range. Anal. Chem. 90 (13), 8093–8101.
Devle, H., Vetti, I., Naess-Andresen, C.F., Rukke, E.O., Vegarud, G., Ekeberg, D., 2012. A comparative study of fatty acid profiles in ruminant and non-ruminant milk. Eur. J. Lipid Sci. Technol. 114, 1036–1043.
Fahy, E., Subramaniam, S., Brown, H.A., Glass, C.K., Merrill Jr., A.H., Murphy, R.C., Raetz, C.R., Russell, D.W., Seyama, Y., Shaw, W., Shimizu, T., Spener, F., van Meer, G., VanNieuwenhze, M.S., White, S.H., Witztum, J.L., Dennis, E.A., 2005. A comprehensive classification system for lipids. J. Lipid Res. 46 (5), 839–861.
Fahy, E., Subramaniam, S., Murphy, R.C., Nishijima, M., Raetz, C.R., Shimizu, T., Spener, F., van Meer, G., Wakelam, M.J., Dennis, E.A., 2009. Update of the LIPID MAPS comprehensive classification system for lipids. J. Lipid Res. 50 (Suppl), S9–14.
Folch, J., Lees, M., Sloane Stanley, G.H., 1957. A simple method for the isolation and purification of total lipides from animal tissues. J. Biol. Chem. 226 (1), 497–509.
Godzien, J., Ciborowski, M., Martinez-Alcazar, M.P., Samczuk, P., Kretowski, A., Barbas, C., 2015. Rapid and reliable identification of phospholipids for untargeted metabolomics with LC-ESI-QTOF-MS/MS. J. Proteome Res. 14 (8), 3204–3216.
Han, X., Gross, R.W., 1995. Structural determination of picomole amounts of phospholipids via electrospray ionization tandem mass spectrometry. J. Am. Soc. Mass Spectrom. 6 (12), 1202–1210.
Han, X., Gross, R.W., 2005. Shotgun lipidomics: electrospray ionization mass spectrometric analysis and quantitation of cellular lipidomes directly from crude extracts of biological samples. Mass Spectrom. Rev. 24 (3), 367–412.
Han, X., Yang, K., Yang, J., Fikes, K.N., Cheng, H., Gross, R.W., 2006. Factors influencing the electrospray intrasource separation and selective ionization of glycerophospholipids. J. Am. Soc. Mass Spectrom. 17 (2), 264–274.
Hara, A., Radin, N.S., 1978. Lipid extraction of tissues with a low-toxicity solvent. Anal. Biochem. 90 (1), 420–426.
Harayama, T., Riezman, H., 2018. Understanding the diversity of membrane lipid composition. Nat. Rev. Mol. Cell Biol. 19 (5), 281–296.
Inloes, J.M., Jing, H., Cravatt, B.F., 2018. The spastic paraplegia-associated Phospholipase DDHD1 is a primary brain phosphatidylinositol lipase. Biochemistry 57 (39), 5759–5767.
Juraschek, R., Dulcks, T., Karas, M., 1999. Nanoelectrospray–more than just a minimized-flow electrospray ionization source. J. Am. Soc. Mass Spectrom. 10 (4), 300–308.
Koivusalo, M., Haimi, P., Heikinheimo, L., Kostiainen, R., Somerharju, P., 2001. Quantitative determination of phospholipid compositions by ESI-MS: effects of acyl chain length, unsaturation, and lipid concentration on instrument response. J. Lipid Res. 42 (4), 663–672.
Lehmann, W.D., Koester, M., Erben, G., Keppler, D., 1997. Characterization and quantification of rat bile phosphatidylcholine by electrospray-tandem mass spectrometry. Anal. Biochem. 246 (1), 102–110.
Liebisch, G., Vizcaino, J.A., Kofeler, H., Trotzmuller, M., Griffiths, W.J., Schmitz, G., Spener, F., Wakelam, M.J., 2013. Shorthand notation for lipid structures derived from mass spectrometry. J. Lipid Res. 54 (6), 1523–1530.
Matyash, V., Liebisch, G., Kurzchalia, T.V., Shevchenko, A., Schwudke, D., 2008. Lipid extraction by methyl-tert-butyl ether for high-throughput lipidomics. J. Lipid Res. 49 (5), 1137–1146.
McMahon, H.T., Boucrot, E., 2015. Membrane curvature at a glance. J. Cell. Sci. 128 (6), 1065–1070.
Milovanovic, D., Honigmann, A., Koike, S., Gottfert, F., Pahler, G., Junius, M., Mullar, S., Diederichsen, U., Janshoff, A., Grubmuller, H., Risselada, H.J., Eggeling, C., Hell, S.W., van den Bogaart, G., Jahn, R., 2015. Hydrophobic mismatch sorts SNARE proteins into distinct membrane domains. Nat. Commun. 6, 5984.
Murray, D.H., Tamm, L.K., 2011. Molecular mechanism of cholesterol- and polyphosphoinositide-mediated syntaxin clustering. Biochemistry 50 (42), 9014–9022.
Paltauf, F., 1994. Ether lipids in biomembranes. Chem. Phys. Lipids 74 (2), 101–139.
Quehenberger, O., Armando, A.M., Brown, A.H., Milne, S.B., Myers, D.S., Merrill, A.H., Bandyopadhyay, S., Jones, K.N., Kelly, S., Shaner, R.L., Sullards, C.M., Wang, E., Murphy, R.C., Barkley, R.M., Leiker, T.J., Raetz, C.R., Guan, Z., Laird, G.M., Six, D.A., Russell, D.W., McDonald, J.G., Subramaniam, S., Fahy, E., Dennis, E.A., 2010. Lipidomics reveals a remarkable diversity of lipids in human plasma. J. Lipid Res. 51 (11), 3299–3305.
Reis, A., Rudnitskaya, A., Blackburn, G.J., Mohd Fauzi, N., Pitt, A.R., Spickett, C.M., 2013. A comparison of five lipid extraction solvent systems for lipidomic studies of human LDL. J. Lipid Res. 54 (7), 1812–1824.
Schafer, L.V., de Jong, D.H., Holt, A., Rzepiela, A.J., de Vries, A.H., Poolman, B., Killian, J.A., Marrink, S.J., 2011. Lipid packing drives the segregation of transmembrane helices into disordered lipid domains in model membranes. Proc Natl Acad Sci U S A 108 (4), 1343–1348.
Schmidt, A., Karas, M., Dulcks, T., 2003. Effect of different solution flow rates on analyte ion signals in nano-ESI MS, or: when does ESI turn into nano-ESI? J. Am. Soc. Mass Spectrom. 14 (5), 492–500.
Schuhmann, K., Herzog, R., Schwudke, D., Metelmann-Strupat, W., Bornstein, S.R., Shevchenko, A., 2011. Bottom-up shotgun lipidomics by higher energy collisional dissociation on LTQ Orbitrap mass spectrometers. Anal. Chem. 83 (14), 5480–5487.
Schuhmann, K., Almeida, R., Baumert, M., Herzog, R., Bornstein, S.R., Shevchenko, A., 2012. Shotgun lipidomics on a LTQ Orbitrap mass spectrometer by successive switching between acquisition polarity modes. J. Mass Spectrom. 47 (1), 96–104.
Schwudke, D., Schuhmann, K., Herzog, R., Bornstein, S.R., Shevchenko, A., 2011. Shotgun lipidomics on high resolution mass spectrometers. Cold Spring Harb. Perspect. Biol. 3 (9), a004614.
Sharpe, H.J., Stevens, T.J., Munro, S., 2010. A comprehensive comparison of transmembrane domains reveals organelle-specific properties. Cell 142 (1), 158–169.
Shevchenko, A., Simons, K., 2010. Lipidomics: coming to grips with lipid diversity. Nat. Rev. Mol. Cell Biol. 11 (8), 593–598.
van den Bogaart, G., Meyenberg, K., Risselada, H.J., Amin, H., Willig, K.I., Hubrich, B.E., Dier, M., Hell, S.W., Grubmuller, H., Diederichsen, U., Jahn, R., 2011. Membrane protein sequestering by ionic protein-lipid interactions. Nature 479 (7374), 552–555.
Wilm, M., 2011. Principles of electrospray ionization. Mol. Cell Proteomics 10 (7) M111 009407.
Wilm, M., Mann, M., 1996. Analytical properties of the nanoelectrospray ion source. Anal. Chem. 68 (1), 1–8.
Yergey, J., Heller, D., Hansen, G., Cotter, R.J., Fenselau, C., 1983. Isotopic distributions in mass-spectra of large molecules. Anal. Chem. 55 (2), 353–356.
Yetukuri, L., Ekroos, K., Vidal-Puig, A., Oresic, M., 2008. Informatics and computational strategies for the study of lipids. Mol. Biosyst. 4 (2), 121–127.